

## **Study on Microstructure and Properties of $\text{Al}_2\text{O}_3/(\text{W},\text{Ti})\text{C}$ Self-Lubricating Tool Material with the Addition of $\text{Al}(\text{OH})_3$ Coated $\text{CaF}_2$**

\*C.C. Sheng, \*M.D. Yi, \*G.C. Xiao, \*M. Li, \*\*C.H. Xu

\*School of Mechanical and Automotive Engineering, Qilu University of Technology, Jinan  
250353, China (xch@qlu.edu.cn)

\*\*School of Mechanical Engineering, Shandong University, Jinan 250061, China

### **Abstract**

$\text{Al}(\text{OH})_3$  coated  $\text{CaF}_2$  powders were prepared by liquid phase coating method with heterogeneous nucleation principle.  $\text{Al}_2\text{O}_3/(\text{W},\text{Ti})\text{C}$  self-lubricating tool material was prepared with the addition of the  $\text{Al}(\text{OH})_3$  coated  $\text{CaF}_2$  powders. The mechanical properties of self-lubricating tool materials with different contents of the coated powders were investigated. The results indicate that the best mechanical properties of the tool material were obtained when the volume content of  $\text{Al}(\text{OH})_3$  coated  $\text{CaF}_2$  was 10%. Compared to its counterpart tool material with uncoated powders, hardness, fracture toughness and flexural strength were increased by 21.7%, 8% and 10.7% respectively. Scanning electron microscope (SEM) was used to observe and analyze the microstructure of tool materials. The result shows that mixed intergranular fracture and transgranular fracture is fracture modes of the tool materials. The cutting tests were carried out using the prepared ceramic cutting tools, which show good wear resistance and antifriction property.

## Keywords

Heterogeneous nucleation, Self-lubricating tool, Microstructure, Mechanical properties, Cutting performance.

## 1. Introduction

With the rapid development of high speed machining technology, it is impossible to meet the production demand just by adding cutting fluid to reduce the cutting temperature [1-3]. The research and application of self-lubricating cutting tool provide a new selection for high speed machining. The significance of achieving self-lubricating for cutting tool material is that it can decrease friction, reduce wear and save the cooling lubricating system. In addition, it can overcome the secondary contamination caused by cutting fluid and improve the ability to protect environment effectively [4-6].

In recent years, the research on the surface coated self-lubricating ceramic cutting tools with good lubricating properties has attracted researchers' attention and has obtained some progress [7-9]. Yan et al. [10] prepared Co-based alloy/TiC/CaF<sub>2</sub> self-lubricating coatings on copper by the method of laser cladding. Pandey et al. [11] prepared CaF<sub>2</sub> thin films by electron beam evaporation technique at room temperature and in a vacuum environment. Shi et al. [12] prepared CaF<sub>2</sub>-coated LiMn<sub>1/3</sub>Ni<sub>1/3</sub>Co<sub>1/3</sub>O<sub>2</sub> particles used for cathode material via a wet chemical process followed by a low-temperature annealing process. Powder coating technology is introduced to the preparation of self-lubricating ceramic cutting tool. It can coat solid lubricant particles, which shows poor performance, with ceramic material, which has excellent mechanical properties. Thereby it can reduce the effect of solid lubricant on the mechanical properties of cutting tool material and maintain the self-lubricating effect of the cutting tool.

In this work, the material design concept of particles surface coating technology was introduced to the research and development of self-lubricating ceramic cutting tools. Coated ceramic self-lubricating cutting tools with self-lubricating properties and improved mechanical properties were fabricated. The combination of lubrication properties and mechanical properties was realized. Moreover, mechanical properties, cutting performance and microstructures of the cutting tool material were studied in detail.

## 2. Experimental Procedure

### 2.1 Preparation of Al(OH)<sub>3</sub> Coated CaF<sub>2</sub> Powders

In this study, core-shell structured Al(OH)<sub>3</sub> coated CaF<sub>2</sub> powders (denoted by CaF<sub>2</sub>@Al(OH)<sub>3</sub>) were prepared by heterogeneous nucleation method. The raw materials used in the experiment are listed in Table 1.

Tab. 1. Raw Materials of Experiment

Name	Chemical formula	Purity
Aluminum nitrate nonahydrate	Al(NO <sub>3</sub> ) <sub>3</sub> ·9H <sub>2</sub> O	99%
Ammonia	NH <sub>3</sub> H <sub>2</sub> O	Analytically pure
Anhydrous ethanol	CH <sub>3</sub> CH <sub>2</sub> OH	Analytically pure
Calcium fluoride	CaF <sub>2</sub>	99%

Powders preparation procedure is as follows: (1) Put a certain amount of Al(NO<sub>3</sub>)<sub>3</sub>·9H<sub>2</sub>O into deionized water, stirring them by a magnetic stirrer until complete dissolution. (2) Put a certain amount of milled CaF<sub>2</sub> powders into a beaker and mix them with deionized water. (3) CaF<sub>2</sub> solution was dispersed uniformly with the ultrasonic disperser and at the same time heated to a certain temperature in the water bath, adding polyethylene glycol (PEG) as surface dispersant. (4) Stir the preceding CaF<sub>2</sub> solution by the DF-II digital display collector magnetic stirrer, dropping ammonia slowly until a small amount of white floe appears. (5) When dropping finished, continue stirring and insulation 30min. (6) After the reaction was completed, the solution aged 12h at room temperature. (7) The suspension was repeatedly washed with deionized water followed by anhydrous ethanol 2 to 3 times, then centrifuged by centrifuge at 2000 rpm for 10 min. To complete the process, it was dried in a vacuum oven at 100°C for 12 h to obtain CaF<sub>2</sub>@Al(OH)<sub>3</sub> powders.

Microstructures of the as-prepared Al(OH)<sub>3</sub> coated CaF<sub>2</sub> powders were observed by SEM (SUPRA<sup>TM</sup>55, Carl Zeiss Group, Germany) and the composition was analyzed using energy

dispersive spectrometry (EDS, SUPRA™ 55, Carl Zeiss Group, Germany).

## 2.2 Preparation of Self-lubricating Tool Materials

The  $\alpha$ -Al<sub>2</sub>O<sub>3</sub> powders (99.9% pure) with an average particle size of 1 $\mu$ m was chosen as the matrix materials. The (W,Ti)C powders (99.8% pure) with an average particle size of 1 $\mu$ m were used as the reinforcing phase. Powders of CaF<sub>2</sub>@Al(OH)<sub>3</sub> have been obtained by experiment with an average particle size of 3-5 $\mu$ m. MgO and NiO were used as sintering additives. The volume ratio of Al<sub>2</sub>O<sub>3</sub> and (W,Ti)C is 1.2:1. Using wet dispersing method to mix materials, drying and sieving powders then filling, cold press molding and hot-pressing sintering under the vacuum state to prepare coated self-lubricating cutting tool material (Al<sub>2</sub>O<sub>3</sub>/(W,Ti)C/(CaF<sub>2</sub>@Al(OH)<sub>3</sub>)). Sintering parameters are as follows: heating rate is 15°C/min, holding temperature is 1650°C for 30 min, hot-pressing pressure is 25 MPa. The volume fraction of CaF<sub>2</sub>@Al(OH)<sub>3</sub> was 5%, 10% and 15%, respectively. Microstructures of the as-prepared cutting tool material was observed by SEM and the phase compositions of cutting tool material was analyzed using X-ray diffraction (XRD, Innov-X System, USA). The sample to be tested is placed in the center of the Cu target, regulating instrument equipment until voltage is 40kV and current is 40mA. The scanning speed is set to 0.4°/min; the range of scanning angle is adjusted to 20°~80°.

## 2.3 Mechanical Properties Tests of Cutting Tool Materials

The as-prepared Al<sub>2</sub>O<sub>3</sub>/(W,Ti)C/(CaF<sub>2</sub>@Al(OH)<sub>3</sub>) ceramic disks were cut into bars with an inner-circular cutter. The bars were ground and then polished to obtain test specimens with 3mm×4 mm×30 mm in dimension. The flexural strength was determined by three-point-bending technique with a span of 20 mm at a crosshead speed of 0.5 mm/min. The hardness was measured using a Vickers hardness tester (Hv-120) with a load of 196 N and loading time of 15 s. The fracture toughness was evaluated by the indentation method using cracks generated by the Vickers indentations. Five specimens for each ceramic disk were tested and the average values of flexural strength, hardness and fracture toughness were taken.

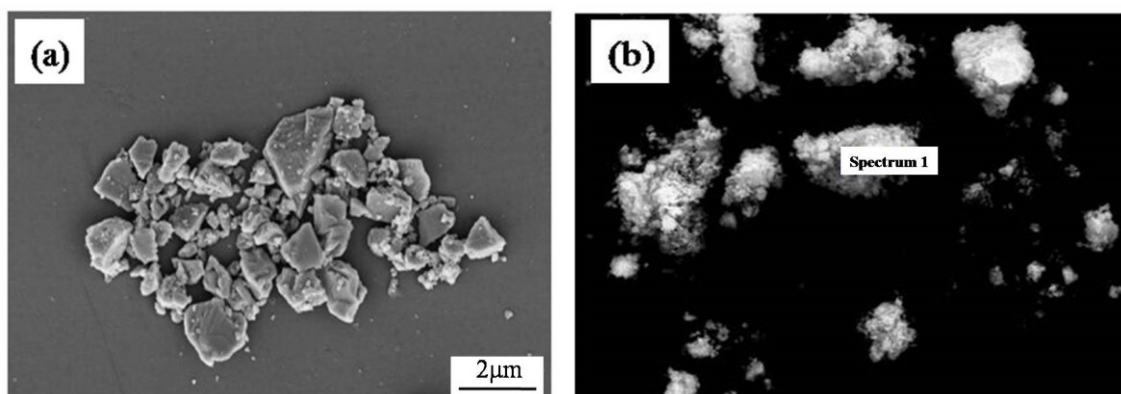
## 2.4 Cutting Experiment of Cutting Tools

Cutting tests were carried out on a CDE6140A lathe under dry cutting condition. The geometric parameters of  $\text{Al}_2\text{O}_3/(\text{W,Ti})\text{C}/(\text{CaF}_2@\text{Al}(\text{OH})_3)$  self-lubricating tool are as follows: rake angle  $\gamma_0 = -8^\circ$ ; relief angle  $\alpha_0 = 8^\circ$ ; inclination angle  $\lambda_s = 0^\circ$ ; cutting edge angle  $\kappa_r = 45^\circ$ ; chamfering width  $b_{\gamma_1} = 0.2\text{mm}$ ; chamfering angle  $\gamma_{o1} = -20^\circ$ ; corner radius  $r_\varepsilon = 0.2\text{mm}$ . The workpiece material was 45# hardened carbon steel with hardness of HRC 25~27. The machining process was performed at a constant feed rate of 0.1 mm/r and a constant depth of cut of 0.2mm. Workpieces were machined at the cutting speed of 60 m/min, 80 m/min and 110 m/min, respectively. The wear morphologies of cutting tools was observed and analyzed by SEM.

## 3. Results and Discussion

### 3.1 Microstructural Characterization of Cutting Tool Materials

SEM images of  $\text{Al}(\text{OH})_3$  coated  $\text{CaF}_2$  in comparison with uncoated ones are shown in Fig.1. It can be seen that coated powders' surfaces become coarse, as shown in Fig.1 (b) and (c) because of  $\text{Al}(\text{OH})_3$  nucleation growths. It is found in Fig.1 (d) that many Al and O elements appear on the powders surface through EDS analysis. Combined with the coating reaction equation (1), it is considered that the surface of the powders were coated with a layer of  $\text{Al}(\text{OH})_3$ .



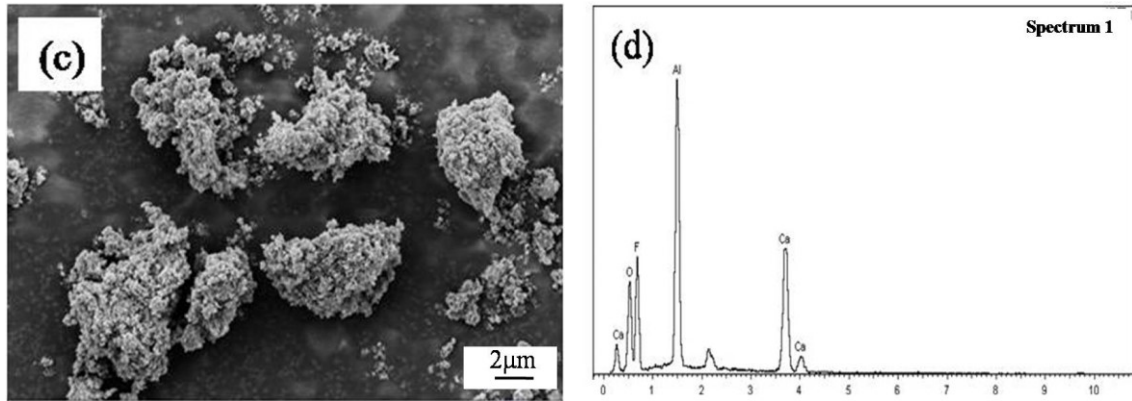


Fig.1 (a) SEM Micrographs of Raw CaF<sub>2</sub> Powders; (b) (c) Coated CaF<sub>2</sub> Powders; (d) EDS Analysis Corresponding to Spectrum 1



Fig.2 presents XRD image of the Al<sub>2</sub>O<sub>3</sub>/(W,Ti)C/(CaF<sub>2</sub>@Al(OH)<sub>3</sub>) self-lubricating tool material. It can be observed that tool materials contain CaF<sub>2</sub> and no derivatives are found. So all the components in the matrix were retained after sintering and CaF<sub>2</sub> did not react with the matrix material. During the sintering process, the coating layer of Al(OH)<sub>3</sub> decomposed into Al<sub>2</sub>O<sub>3</sub>, which is expressed as reaction equation (2). Therefore, no Al(OH)<sub>3</sub> was detected in Fig. (2).

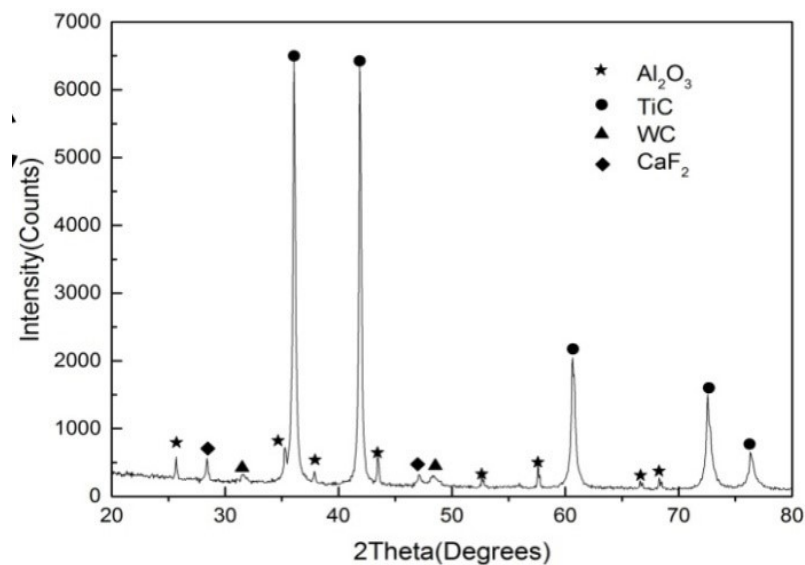


Fig.2. XRD Spectrum of Al<sub>2</sub>O<sub>3</sub>/(W,Ti)C/(CaF<sub>2</sub>@Al(OH)<sub>3</sub>) Self-lubricating Tool Material

Fig.3 shows the polished surfaces of self-lubricating tool material with different contents of  $\text{CaF}_2@Al(OH)_3$ . The white is identified by EDS to be  $(W,Ti)C$ , and the black is  $Al_2O_3$  and  $\text{CaF}_2@Al(OH)_3$ . The distribution of each component of the cutting tool material is even, and the grain arrangement is compact and the particles are wrapped with each other can be found, as seen in Fig.3.

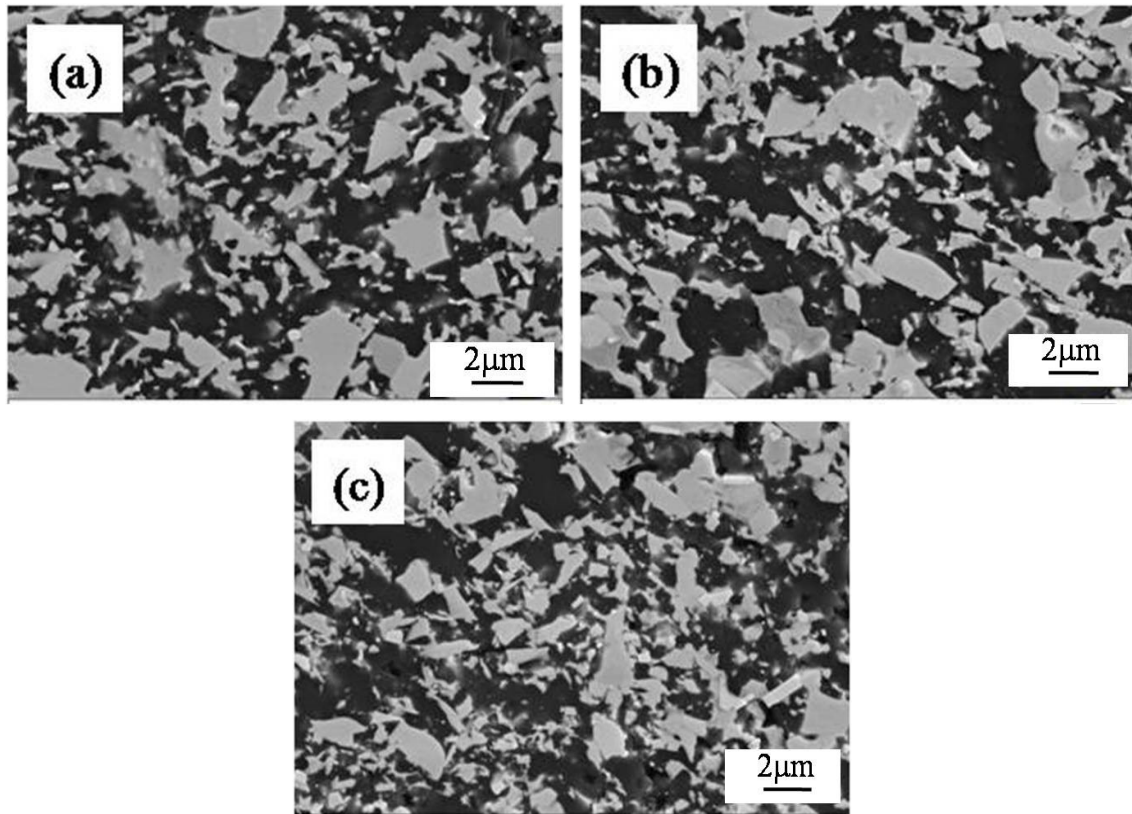


Fig.3. SEM Micrographs of Polished Surfaces of Self-lubricating Tool Material with Different Volume Contents of  $\text{CaF}_2@Al(OH)_3$ : (a) 5%; (b) 10%; (c) 15%

Fig.4 shows the fracture surface of the self-lubricating tool material with different contents of  $\text{CaF}_2@Al(OH)_3$ . It can be seen that the tool material particle is larger and the density is poor when the volume content of  $\text{CaF}_2@Al(OH)_3$  is 5%, as shown in Fig.4 (a). The particle distribution of each component of the cutting tool material is uniform and more dense when the volume content of  $\text{CaF}_2@Al(OH)_3$  is 10%, as shown in Fig.4 (b). Tool material particle is larger and the distribution is uneven when the volume content of  $\text{CaF}_2@Al(OH)_3$  is 15%, as shown in Fig.4 (c). There is a pore in the fracture surface of the tool material, which is judged to be left after the grain was pulled out. This phenomenon is a typical intergranular fracture. At the same

time, there are some steps in the morphological appearance, which is judged to be formed after the grain fracture. This phenomenon is a typical transgranular fracture. Therefore, mixed transgranular fracture and intergranular fracture is fracture modes for the self-lubricating ceramic cutting tool materials. This model is helpful to improve the strength of the cutting tool materials.

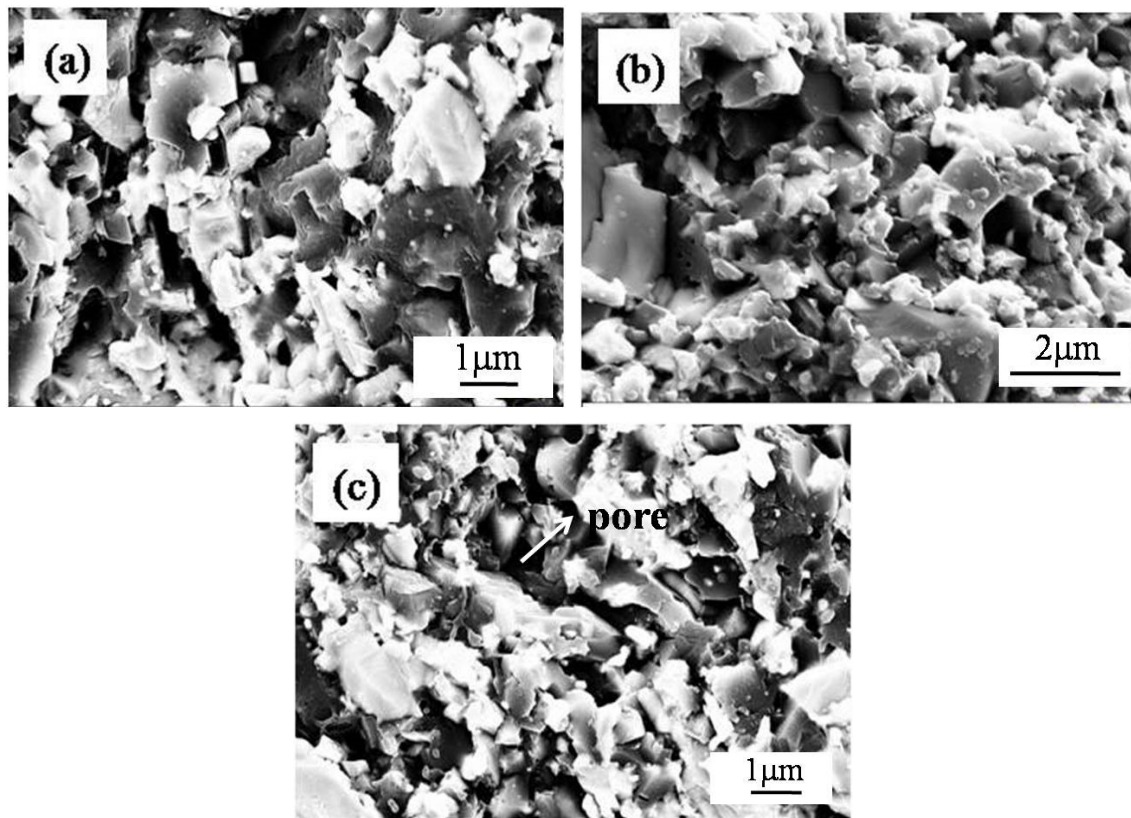


Fig.4. SEM Micrographs of Fracture Surfaces of the Self-lubricating Tool Material with Different Volume Contents of  $\text{CaF}_2@Al(OH)_3$ : (a) 5%; (b) 10%; (c) 15%

### 3.2 Mechanical Properties of Cutting Tool Materials

Fig.5 (a) shows the effect of  $\text{CaF}_2@Al(OH)_3$  content on the hardness of tool material. It can be seen that with the increase of the content of  $\text{CaF}_2@Al(OH)_3$ , the hardness of the cutting tool material decreases gradually. The hardness of the tool material is 16.98 GPa when the volume content of  $\text{CaF}_2@Al(OH)_3$  is 5%, while the hardness is 14.67 GPa with the addition of 15%, declined 15.7%, as shown in Fig.5 (a). With the increase of the content of  $\text{CaF}_2@Al(OH)_3$ , the fracture toughness of the cutting tool material increases first and then decreases as shown in Fig.5 (b). When the volume content is 10%, the fracture toughness is  $4.12 \text{ MPa}\cdot\text{m}^{1/2}$ . The flexural



strength values show a similar tendency as the fracture toughness, which can be seen in Fig.5 (c) that the flexural strength is 607 MPa when the volume content is 10%.

In summary, the best mechanical properties of the tool material can be achieved when the volume content of  $\text{CaF}_2@Al(OH)_3$  is 10%, which the hardness, fracture toughness and flexural strength are 16.03 GPa,  $4.12 \text{ MPa}\cdot\text{m}^{1/2}$  and 607 MPa, respectively.

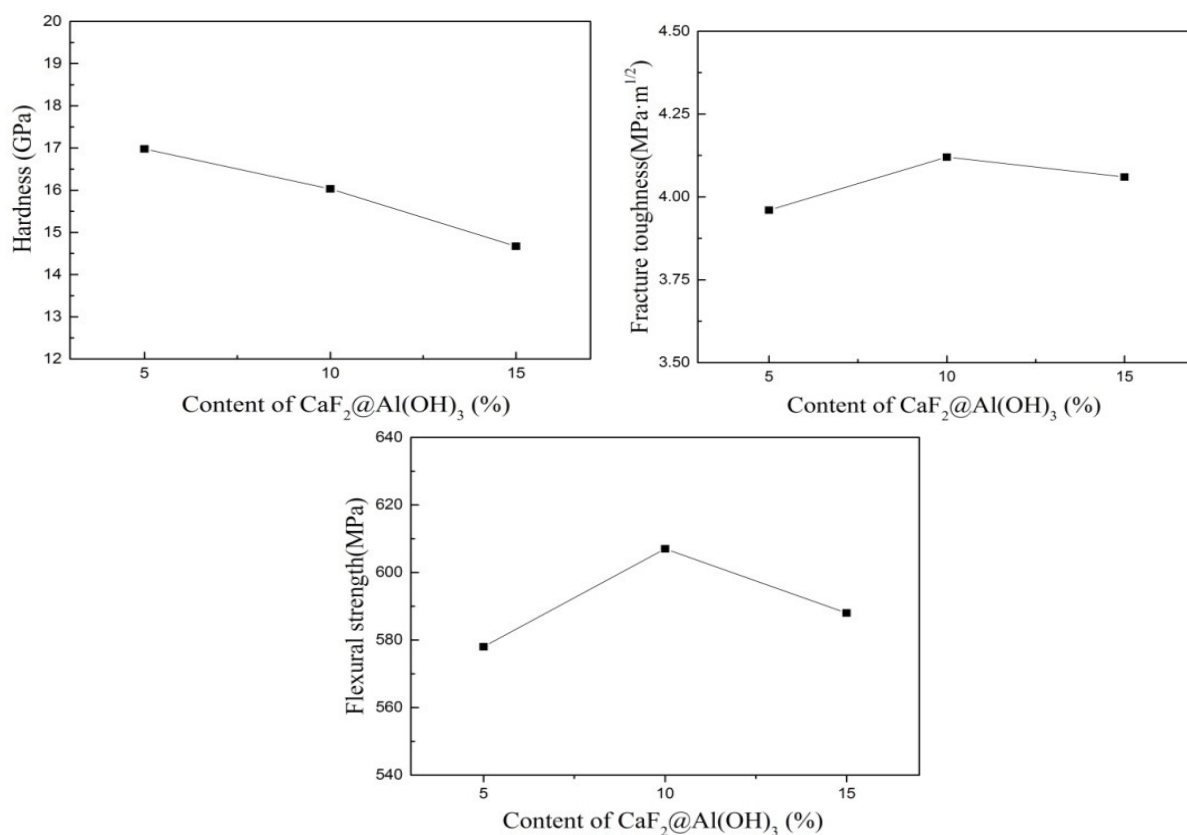


Fig.5. The Effect of  $\text{CaF}_2@Al(OH)_3$  Content on Mechanical Properties of Tool Materials

Mechanical properties of the self-lubricating ceramic cutting tool materials with the addition of  $Al(OH)_3$  coated  $\text{CaF}_2$  and uncoated  $\text{CaF}_2$  are listed in Table 2 for comparison. The hardness, fracture toughness and flexural strength of the  $Al_2O_3/(W,Ti)C/(CaF_2@Al(OH)_3)$  material were increased by about 21.7%, 8% and 10.7%, respectively, as compared with the corresponding uncoated  $\text{CaF}_2$  material. The similar results can be obtained according to other studies. Chen et al. [13] prepared  $Al_2O_3/TiC(h-BN@SiC)$  self-lubricating ceramic tool materials. When  $h-BN@SiC$  powders was 5 vol.%, the tool material's hardness and fracture toughness are 12.8% and 44.4% higher than that of  $Al_2O_3/TiC/h-BN$  tool material.

Tab. 2. Mechanical Properties of the Ceramic with Coated CaF<sub>2</sub> Powders Compared with Uncoated CaF<sub>2</sub> Powders

Property index	Uncoated CaF <sub>2</sub> Powders		Increment (%)
	Adding coated CaF <sub>2</sub> powders	Adding uncoated CaF <sub>2</sub> powders	
Hardness (GPa)	16.03	13.17	21.7
Fracture toughness (MPa·m <sup>1/2</sup> )	4.12	3.81	8
Flexural strength (MPa)	607	549	10.7

### 3.3 Cutting Performances of Cutting Tool

Fig.6 shows the relationship between cutting tool life and cutting speed when cutting 45# steel. The depth of cut and feed rate are constant, and the standard of tool blunt VB is 0.3mm. With the increase of cutting speed, tool life increases first and then decreases as shown in Fig.6. Because the solid lubricant cannot be dragged to form lubricating film when the cutting speed is lower ( $v=60\text{m/min}$ ), it is bad for tool cutting. The result is the tool wear becomes faster and the tool life becomes shorter. When the cutting speed is higher ( $v=80\text{m/min}$ ), solid lubricant is more conducive to form lubricating film. It can effectively improve the wear resistance of the tool and improve the tool life.

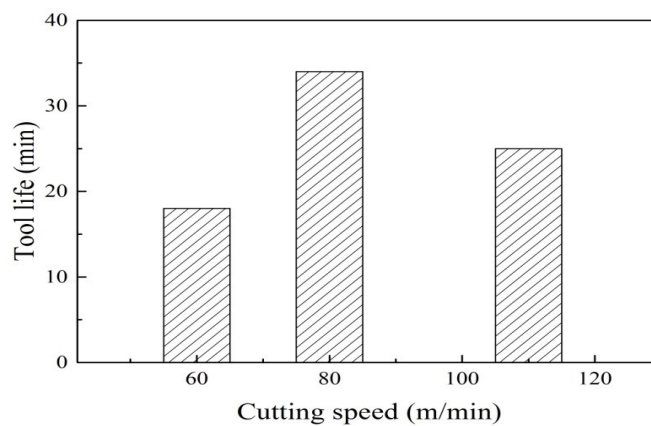


Fig.6 The Relationship between Tool Life and Cutting Speed

Fig.7 (a) presents SEM micrographs of rake face wear of self-lubricating tool when cutting 45# steel. It is obviously seen that a furrow appeared on the rake face, which belongs to abrasive wear. But the wear area is small, which indicates that the tool has better wear resistance and adding coated solid lubricant to tool material can improve the cutting performances. Fig.7 (b) presents SEM micrographs of flank wear of self-lubricating tool when cutting 45# steel. It can be seen that the area of mechanical ploughing wear appeared on the flank face and the wear mechanism is abrasive wear.

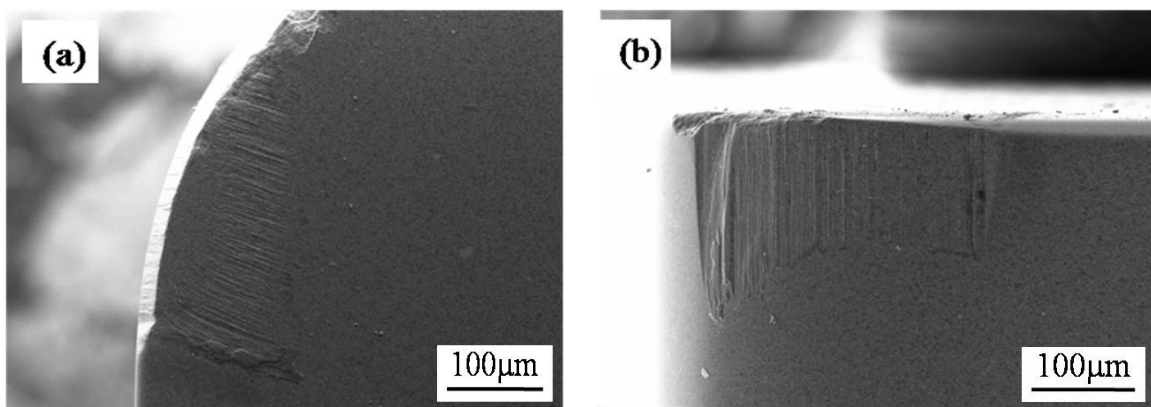
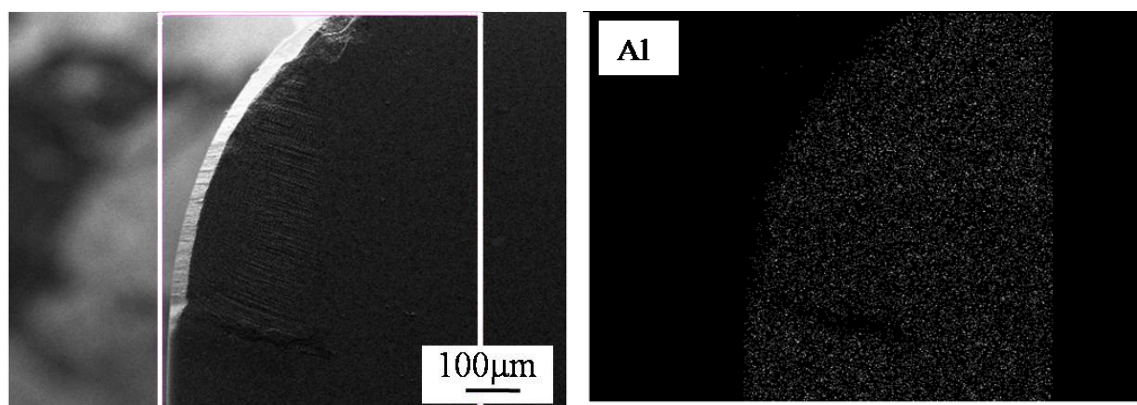


Fig.7. SEM Micrographs of Cutting Tool Wear: (a) Rake Face Wear; (b) Flank Face Wear

Fig.8 presents EDS spectrum analysis of the elemental distribution of the self-lubricating tool rake face and the elements of Al, Fe and Ca are listed respectively. It can be seen that there are a large amount of Fe elements in the wear area of the tool surface, which is caused by iron bonding with the tool surface. The distribution of Al and Ca elements and solid lubricant is homogeneous, which can be in favor to form a uniform lubricating film on rake face in cutting process.



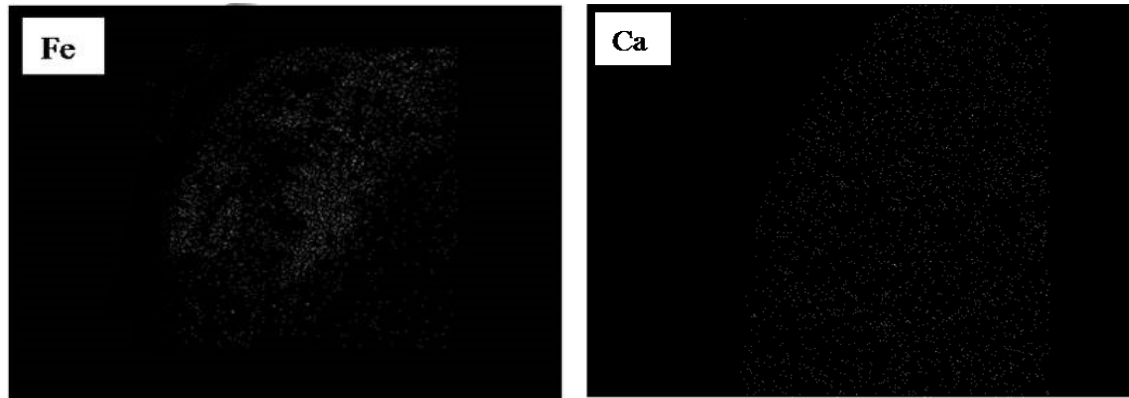


Fig.8. EDS Image of Element Distribution of Tool Rake Face

## Conclusions

A type of self-lubricating ceramic cutting tool material was developed by adding  $\text{Al}(\text{OH})_3$  coated  $\text{CaF}_2$  powders. The main conclusions of this study are as follows:

(1)  $\text{Al}(\text{OH})_3$  coated  $\text{CaF}_2$  powders were prepared successfully and the mechanical properties of the tool material can be improved by adding moderate  $\text{Al}(\text{OH})_3$  coated  $\text{CaF}_2$  powders. The best mechanical properties can be obtained when the volume content of  $\text{CaF}_2@ \text{Al}(\text{OH})_3$  is 10%, the hardness, fracture toughness and flexural strength are 16.03 GPa, 4.12  $\text{MPa}\cdot\text{m}^{1/2}$  and 607 MPa, respectively.

(2) The microstructure of cutting the tool material was observed and analyzed by SEM. The result indicates that the fracture mode of the self-lubricating tool is intergranular fracture and transgranular fracture.

(3) Cutting test shows that the  $\text{Al}_2\text{O}_3/(\text{W},\text{Ti})\text{C}$  self-lubricating tool with  $\text{Al}(\text{OH})_3$  coated  $\text{CaF}_2$  powders has good wear resistance and antifriction property.

## References

1. L.F. Qin, T. Sun, Research and application progresses of dry cutting technology, 2013, Modular Machine Tool & Automatic Manufacturing Technique, vol. 4, pp. 9-12.
2. O.M.M. Silva, J.V.C. Souza, M.D.C.D.A. Nono, et al., Development of ceramic cutting tools for future application on dry machining, 2010, Materials Science Forum, vol. 10, pp. 724-729.
3. C. Xu, Graphitization of diamond powders under hot pressing conditions and the fabrication of toughened ceramics, 2005, AMSE Journals, Modelling A, vol. 78, no. 1-2, pp. 1-10.

4. T. Cao, J. Deng, Self-lubricating mechanism of a self-lubricating ceramic cutting tool, 2006, Kuei Suan Jen Hsueh Pao Journal of the Chinese Ceramic Society, vol. 34, no. 10, pp. 1232-1237, 2006
5. J.X. Deng, T.K. Cao, X. Ai, Friction reducing mechanisms of  $\text{Al}_2\text{O}_3/\text{TiC}/\text{CaF}_2$  self-lubricating ceramic tools in machining processes, 2006, Chinese Journal of Mechanical Engineering, vol. 42, no. 7, pp. 109-113.
6. K. Zhuang, D. Zhu, X. Zhang, et al., Notch wear prediction model in turning of Inconel 718 with ceramic tools considering the influence of work hardened layer, 2014, Wear, vol. 313, no. 1-2, pp. 63-74.
7. H.A. Rashkis, S.R. Rashkis, Development and performance evaluation of self-lubricating drill tools, 2015, ARCHIVE Proceedings of the Institution of Mechanical Engineers Part J Journal of Engineering Tribology, vol. 229, no. 12, pp. 1289-1291.
8. G.Y. Wu, C.H. Xu, G.C. Xiao, et al., "Self-lubricating ceramic cutting tool material with the addition of nickel coated  $\text{CaF}_2$  solid lubricant powders, 2016, International Journal of Refractory Metals and Hard Materials, vol. 56, pp. 51-58.
9. Z.Q. Chen, C.H. Xu, H. Chen, et al., The influence of process parameters on the preparation of  $\text{CaF}_2@(\text{Al}(\text{OH})_3)$  composite powder via heterogeneous nucleation, 2015, International Journal of Material Research, vol. 106, no. 2, pp. 88-191.
10. H. Yan, J. Zhang, P. Zhang, et al, Laser cladding of Co-based alloy/ $\text{TiC}/\text{CaF}_2$ , self-lubricating composite coatings on copper for continuous casting mold, 2013, Surface & Coatings Technology, vol. 232, no. 1, pp. 362-369.
11. R.K. Pandey, M. Kumar, S.A. Khan, et al., Study of electronic sputtering of  $\text{CaF}_2$ , thin films, 2014, Applied Surface Science, vol. 289, no. 2, pp. 77-80.
12. S.J. Shi, J.P. Tu, Y.J. Mai, et al., Structure and electrochemical performance of  $\text{CaF}_2$  coated  $\text{LiMn}_{1/3}\text{Ni}_{1/3}\text{Co}_{1/3}\text{O}_2$  cathode material for Li-ion batteries, 2012, Electrochimica Acta, vol. 83, no. 12, pp. 105-112.
13. H. Chen, C. Xu, G. Xiao, et al., Investigation of  $\text{Al}_2\text{O}_3/\text{TiC}$  ceramic cutting tool materials with the addition of SiC-coated h-BN: preparation, mechanical properties, microstructure and wear resistance, 2016, International Journal of Materials Research, vol. 107, no. 8.